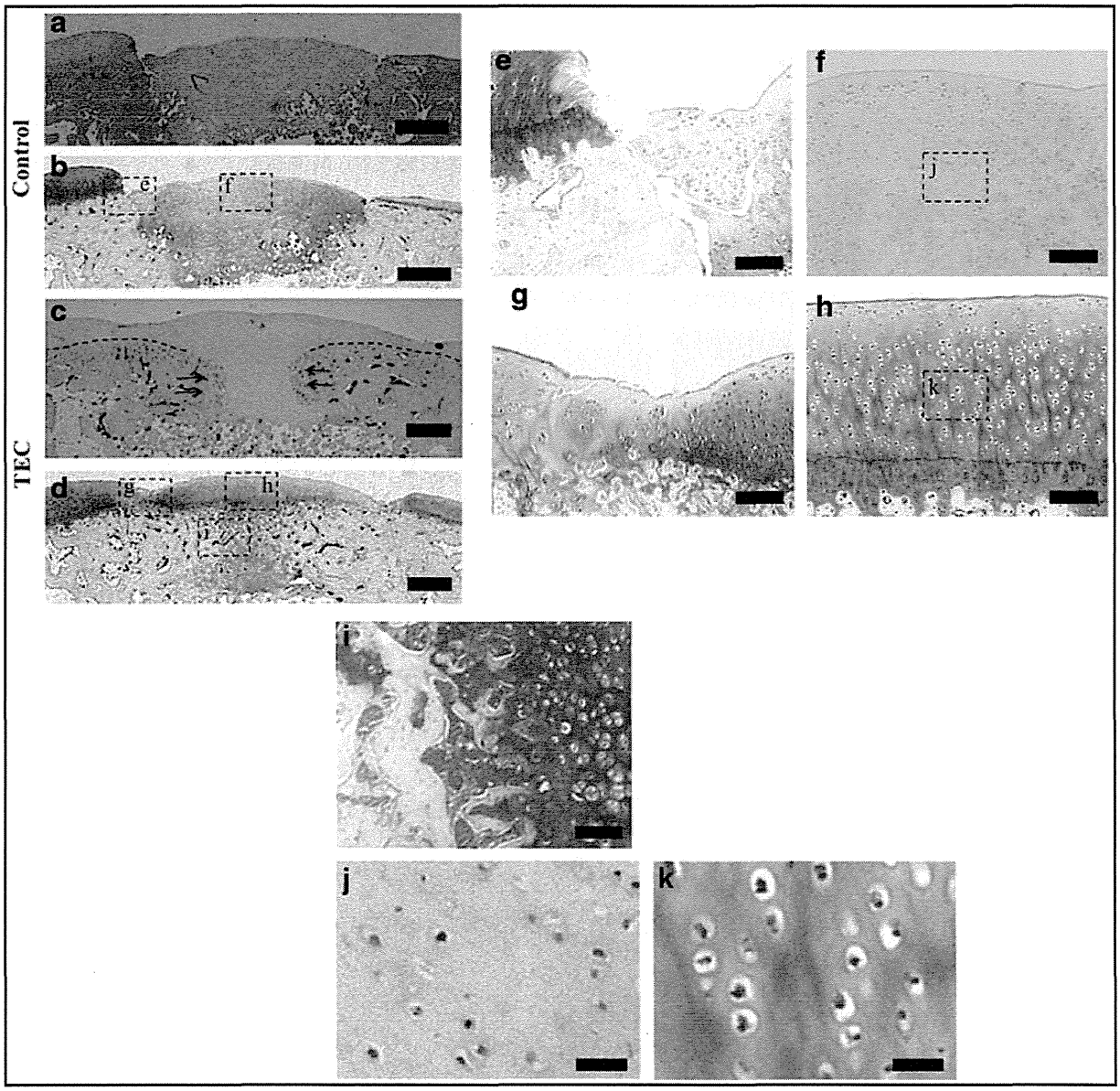

FIG. 4. Hematoxylin and eosin (H&E) staining and Toluidine Blue staining of repair tissues from defects treated with artificial bone alone **(a, b)** or the combined implant **(c, d)**. Bar = 1 mm. Arrows show that new bone formation within the TEC further extended from the bilateral peripheral border toward the central area on the surface of the artificial bone **(c)**. Light magnification view at the border **(e, g)**, center **(f, h)** area of the repair tissue, and cartilage-like tissue in contact with newly synthesized bone **(i)**. Bar = 100 μm. Note that the defect treated with the combined implant was repaired with osteochondral tissue and exhibited good tissue integration to the adjacent host tissue. Higher magnification views at the center area of the repair tissue **(j, k)**. Bar = 20 μm. Cellular morphology of defects treated with the combined implant shows round-shaped cells in lacuna. Color images available online at www.liebertpub.com/tea

exhibited poor integration with the adjacent host cartilage (Fig. 5a, arrows, e). In contrast, the TEC group samples showed complete osteochondral repair (Fig. 5c, d), and good tissue integration of the repair tissue to the adjacent host tissue persisted (Fig. 5c, arrows, g). However, some subjects exhibited overgrowth of the subchondral bone with the thinning of cartilage (Fig. 5c, d). Higher magnification views revealed that the repair tissue and the border with the adjacent cartilage contained a number of cell clusters in the control group, and the distribution of chondrocytes was disorganized throughout the matrix (Fig. 5f, i, j), suggesting the involvement of some pathological condition within the repair tissue and the adjacent host cartilage in this group. Conversely, in the TEC group, the repair tissue exhibited hyaline-like cartilage without cells in clusters, and the chondrocytes were arranged in longitudinal columns in the center area of the samples (Fig. 5h, k, l).

Histological score for cartilage repair

The total histological scores for cartilage repair were significantly higher in the TEC group samples compared with those in the control group at 1 month (14.22 ± 2.02 vs. 5.34 ± 2.59, $p = 0.010$), 2 months (19.16 ± 2.33 vs. $13.67 \pm$

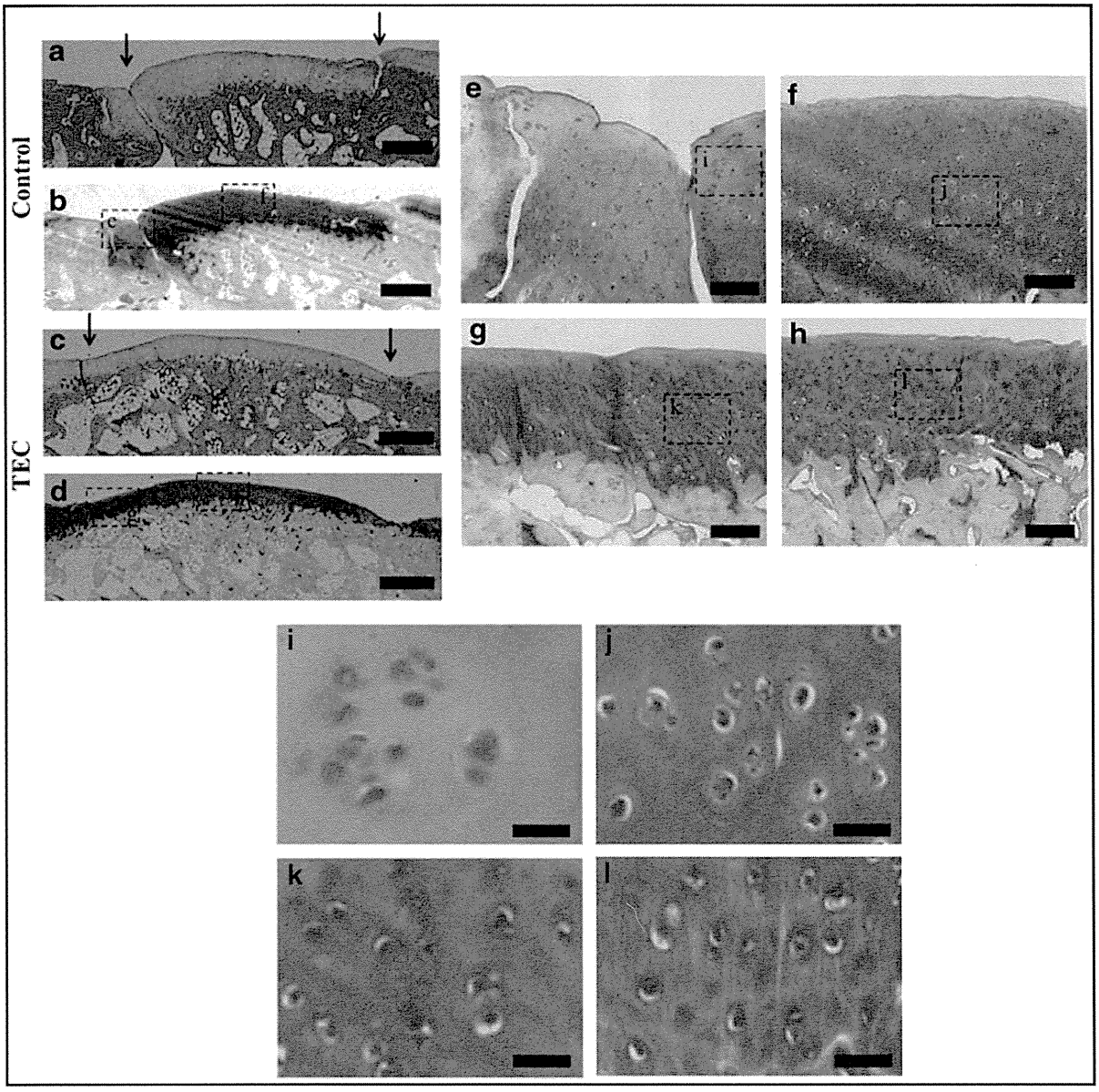

FIG. 5. H&E staining and Toluidine Blue staining of repair tissues treated with artificial bone alone **(a, b)** or the combined implant **(c, d)**. Bar = 1 mm. Light magnification view at the border **(e, g,** arrow) and center **(f, h)** area of the repair tissue. Bar = 100 μm. Note that the repair tissue in defects treated with the combined implant sustained good tissue integration to the adjacent host tissue, while that of artificial bone alone showed poor integration. Higher magnification views at the border **(i, k)** and center areas **(j, l)** of the repair tissue. Bar = 20 μm. Cellular morphology in defects treated with the combined implant showed round-shaped cells in lacuna, while that in defects treated with artificial bone alone showed cell clustering in lacuna. Color images available online at www.liebertpub.com/tea

2.10, $p = 0.018$), and 6 months (19.03 ± 2.15 vs. 9.56 ± 5.17, $p = 0.012$) after surgery (Fig. 6a).

The categories "cellular morphology" and "toluidine blue staining" in the TEC group were significantly higher than those in the control group samples out to 6 months postsurgery, and these results suggested the promotion of cartilage repair with the combined implants. With regard to the category "bonding to adjacent cartilage," the histological scores in the TEC group samples were significantly higher compared with those in the control group throughout the studies. In addition, the category "structural integrity," especially the subcategory "border area," values for the TEC group were significantly higher than those of the control group at 6 months, suggesting that secure integration to adjacent host tissue contributed to the proper development of the border area of the repair cartilage. In contrast, the categories "chondrocyte clustering" and "freedom from degeneration of adjacent cartilage" showed significantly lower scores in the control group at 6 months, findings that suggest the involvement of a pathological process within the repair tissue (Table 1).

Histological score for subchondral bone repair

At 1 month after surgery, subchondral bone repair was not observed in either the TEC group or the control group. Therefore, all categories except for the category "exposure of

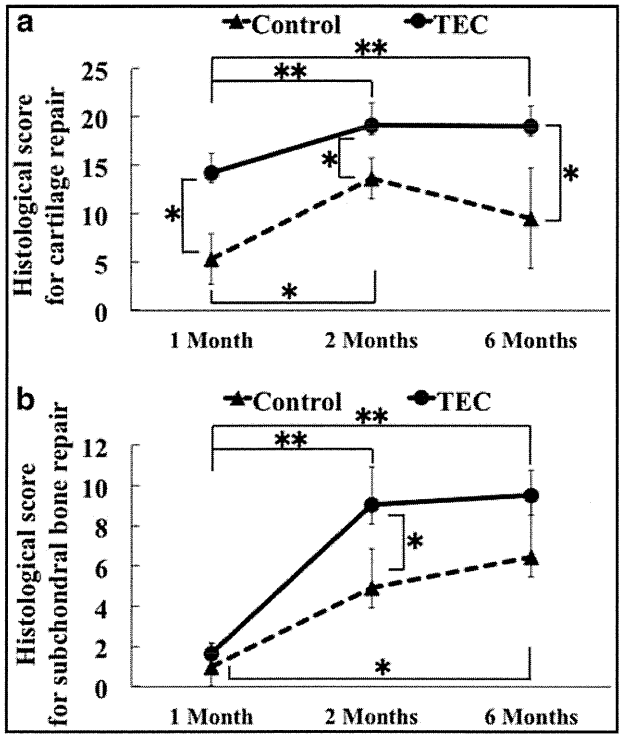

FIG. 6. Modified O'Driscoll scores in the control and TEC groups for cartilage repair **(a)** and subchondral bone repair **(b)** $*p<0.05$, $**p<0.01$. Notably, the combined implants generated from TEC and artificial bone contributed to enhanced osteochondral repair for approximately 6 months after surgery, compared with the control group samples.

subchondral bone" were scored as 0. At 2 months postsurgery, the total histological score for subchondral bone repair was significantly higher in the TEC group than in the control group (9.07 ± 1.84 vs. 4.92 ± 1.91, $p=0.014$). At 6 months, there were no significant differences detected between the two groups (9.54 ± 1.26 vs. 6.47 ± 3.20, $p=0.094$) (Fig. 6b).

In the categories "subchondal bone alignment," "bone integration," "bone infiltration into defect area," and "cellular morphology," there were significant differences between the TEC and the control groups at 2 months post implantation ($p<0.05$). These results implied that the combined implant accelerated subchondral bone repair in the early stages. At 6 months after surgery, only scores for the category "tidemark continuity" in the TEC group were significantly higher than those in the control group. Notably, the category "exposure of subchondral bone" worsened in the control group at 6 months compared with 2 month values (Table 2).

Mechanical properties

The osteochondral repair tissue resulting from implantation with the combined implant restored stiffness values close to those for normal osteochondral tissue (23.2 ± 12.5 vs. 16.8 ± 10.0 mN/m, $p=0.40$), with no significant differences observed between the two groups (Fig. 7).

Discussion

Many therapeutic procedures have been investigated to biologically repair damaged cartilage, some of which are

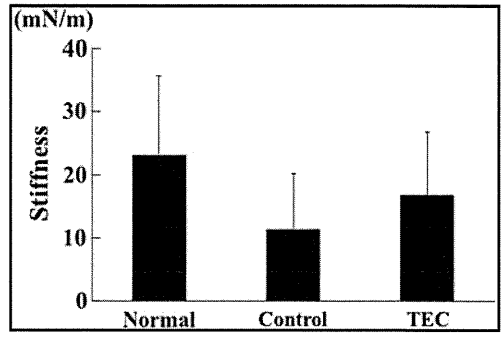

FIG. 7. The stiffness of normal rabbit osteochondral tissue ($N=5$), the control defect group ($N=5$), and the TEC group ($N=5$). The osteochondral repair tissue resulting from the combined implant restored the tissue stiffness to values close to those of normal osteochondral tissue.

already at the stage of clinical application.[30–35] On the other hand, the incidence of OA, which involves subchondral bone pathology, is higher than that of isolated chondral injury.[36–41] Therefore, the development of novel therapeutic methods for osteochondral repair is necessary, considering the large population of OA patients. Recently, tissue engineering approaches have been tested and proved to be efficient in several animal studies[42–46] and clinical trials[5,47–49] using biphasic or triphasic constructs. These constructs should be reasonable for osteochondral repair due to both mechanical and biological reasons such as acquisition of initial mechanical strength, mimicking a natural articular structure, a uniform tidemark at the osteochondral junction, and integration of the implant with host tissue to sustain biological function.[10,13,16,50] On the other hand, no previous study focused on the detailed process of osteochondral repair with time course transitions. Through the comparison of biphasic implant with artificial bone alone, we have demonstrated the significance of the combination of stem cell-based TEC with artificial bone in the process of osteochondral repair.

In the present study, the feasibility of a combined implant consisting of a scaffold-free TEC derived from synovial

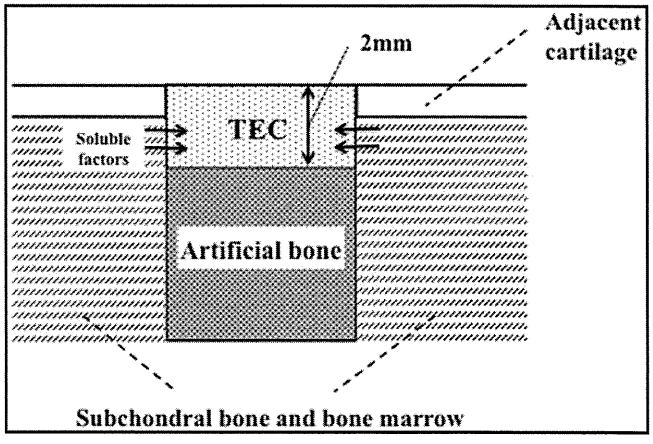

FIG. 8. Schematic representation of the relationship between bone marrow and the depth of the combined implants. The bottom of the TEC on the artificial bone comes into contact with the subchondral bone at the lateral border and, thus, the transport of soluble factors could be expected to be between the TEC and bone marrow.

MSCs and a fully interconnected HA artificial bone (TEC-HA combined implant) to facilitate rabbit osteochondral repair was demonstrated. Being artificial scaffold free, the TEC contained no animal- or chemical-derived materials. The fully interconnected HA has been widely used as a bone substitute in clinical practice.[19,51,52] Moreover, it should be noted that the hybridization of the TEC with the HA artificial bone can be simply accomplished, as it occurs immediately after the contact of these two materials without any reinforcement for fixation, unlike previously reported biphasic materials, which needed some adhesive or glue to combine different materials and required a complicated process of manufacturing implants.[10,17] This stable association led to the development of secure tissue integration between the repair cartilage and subchondral bone as shown by the high O'Driscoll scores out to 6 months post implantation. The tight association between the TEC and the HA artificial bone may be based on the high affinity of HA for glycoproteins that are enriched in these TEC,[22,23] and such a simple and efficient procedure has made it possible to associate these two materials just before use in the surgical model. Taken together, the TEC-HA combined implant could be advantageous not only with regard to safety, but also related to time- and cost effectiveness.

The present study revealed that the TEC-HA combined implant contributed to a significantly superior morphological osteochondral repair out to 6 months after surgery, when compared with the HA artificial bone-alone group. It should be noted that the artificial bone was implanted $\sim$2 mm below the level of the articular surface. Thus, the bottom of the TEC came in contact with the subchondral bone at the lateral border, and, therefore, the transport of soluble factors could be expected between the TEC and bone marrow (Fig. 8). Furthermore, the TEC sealed the entire osteochondral lesion from the articular surface with maintenance of the secure adhesion of the TEC to the adjacent host cartilage. Accordingly, the bone marrow-soluble factors were likely specifically exposed to the lower aspect of the TEC in contact with the adjacent subchondral bone. Under such an environment, it was notable that the complex of osteogenesis and chondrogenesis was initially observed exactly in such lower aspects of the TEC at the lateral border which was in contact with the adjacent subchondral bone at 1 month post implantation of the TEC-HA construct. Remarkably, such reactions were not observed at this point within the repair tissue of the control group in which only the HA block was implanted. The repair tissue in this group was fibrous in nature, although the initial repair tissue developing on the surface of the HA blocks in the control group presumably contained abundant bone marrow-derived MSCs and bone marrow growth factors. Therefore, it is not likely that the co-existence of the bone marrow growth factors with the bone marrow-derived MSCs in the initial clot resulted in the induction of osteochondral tissue at 1 month postsurgery. Synovial-derived MSCs within the TEC can differentiate to develop chondrogenic[22,23] or osteogenic tissue (unpublished data) *in vitro* when cultured in the presence of differentiation stimulating growth factors. Taken together, it is reasonable to speculate that the complex of osteogenic and chondrogenic differentiation responses observed at the lower aspect of the TEC might be mainly attributable to the differentiation of synovial derived MSCs within the TEC which were exposed to the bone marrow osteochondral differentiation factors from the adjacent host subchondral bone. Subsequently, the development of an osteochondral tissue complex extended toward the center area of the TEC to accomplish the repair of the subchondral bone throughout the width of the osteochondral defect. Such progression of the osteochondral tissue development suggests that the newly synthesized osteochondral tissue likely had exerted some paracrine effects which preceded the subsequent osteochondral differentiation within the adjacent TEC in the central portion. Conversely, the progression of repair in the control group with HA-bone alone was significantly slower and likely did not involve rapid osteochondral tissue formation as observed in the TEC group, with incomplete and delayed formation of subchondral bone (Fig. 9a, b). However, such incomplete and delayed subchondral bone repair was not completely reflected by the O'Driscoll scores such as in the category "subchondral bone alignment," and no significant differences were detected between the two groups at 6 months post implantation. This may be based on the scoring system that did not subtract significant scores in the case of "depressed of subchondral bone," and, thus, failed to depict the differences in subchondral repair between the TEC group and the HA-only group.

Taken together, the present study clearly demonstrated that the restoration of subchondral bone was significantly accelerated and promoted in the TEC group as compared with the control group. The restoration of the subchondral bone could directly contribute to the improvements in the mechanical properties of the repair tissue and, therefore, such promotion could potentially lead to the introduction of an accelerated rehabilitation program. This point could be one of the major advantages of the TEC-HA implant in relation to their potential clinical impact.

It should be noted that the repair tissue maintained good tissue integration to the adjacent host cartilage and subchondral bone out to 6 months after surgery in the TEC-HA group, similar to our previous studies in porcine models.[23,24] Conversely, not only poor integration was attained but also exposure of subchondral bone remained in the control group. In other osteochondral repair studies using biphasic scaffolds in a goat model, the repair tissues that were better integrated with native surrounding cartilage exhibited more congruence with the surface of native adjacent cartilage and less fibrillations and irregularities at the surface, accompanied with a higher O'Driscoll score.[46,53] Thus, the tissue integration to native surrounding tissue after implantation could influence the quality and maturation of repair tissue. In addition, extensive clustering of chondrocytes was observed in the repair tissue of the control group animals, although there was development of a cartilage-like tissue in this group at 6 months. Such phenomena were predominant around the cracks between the repair tissue and the adjacent host cartilage. It is likely that the cartilage-like repair tissue which failed to integrate with the adjacent host cartilage might evolve into a pathological condition, which potentially raises concerns regarding the long-term durability of the repair tissue, as cell clustering suggests some ongoing pathological conditions such as is observed in OA,[54–57] and such pathological conditions show mechanical weakness.[58–60] In contrast, no such clustering of chondrocytes was observed

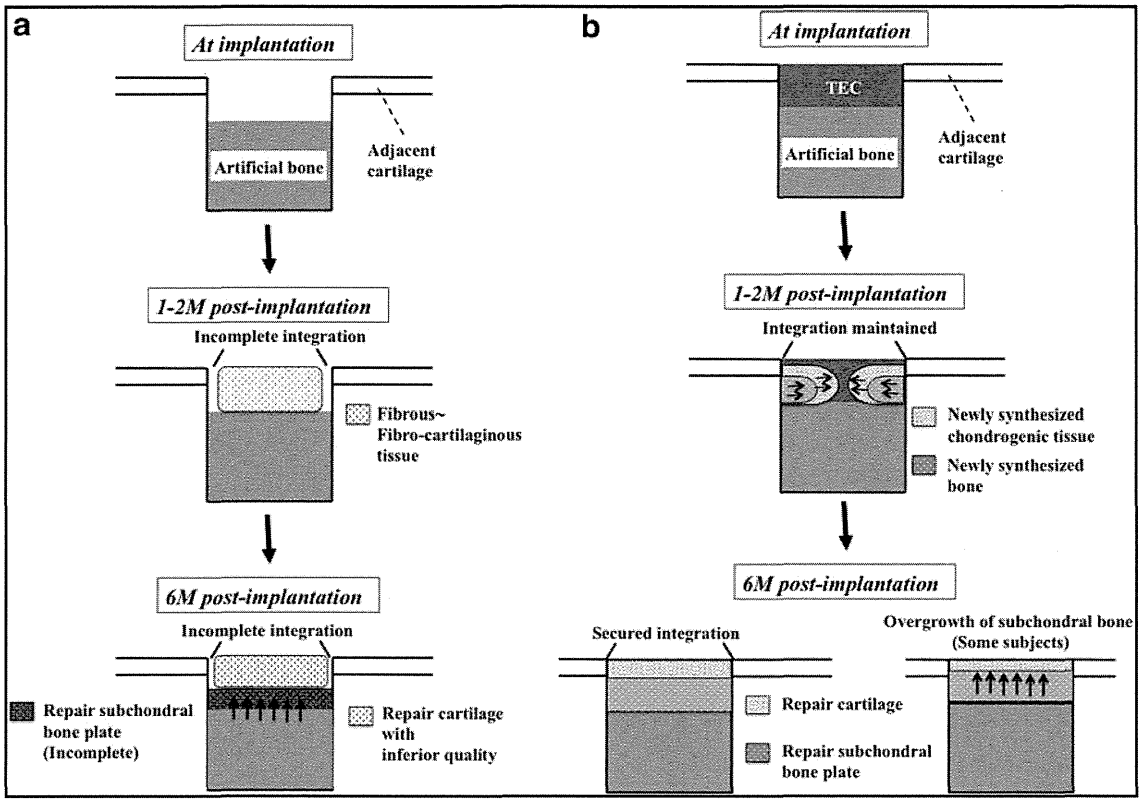

FIG. 9. Schematic representation of the repair process using artificial bone alone **(a)** and the combined implants made with TEC and artificial bone **(b)**. In the bone-alone control group, there appeared to be a phenotypic change from a fibrous tissue to a more fibrocartilaginous or cartailaginous tissue, and delayed formation of subchondral bone. Conversely, the development of an osteochondral tissue complex spreads toward the center area from the bottom of the TEC on the artificial bone in contact with the subchondral bone at the lateral border.

in the repair tissue of the TEC-HA group and rather, chondrocytes in the repair tissue were arranged in longitudinal columns, suggesting some restoration of normal cartilage architecture. Therefore, the TEC-HA implant could foster longer-term durability of the repair cartilage with maintenance of secure tissue integration to the adjacent host tissue, properties that could also be very clinically relevant.

Allogenic cells were used in this study, which may raise a concern regarding immunological rejection. However, recent studies have suggested the immune-tolerance capacity of MSCs by suppressing the activity of immune cells such as T cells.[61,62] Likewise, our results showed that no abnormal inflammatory response or immunological rejection such as macrophage and lymphocyte invasion was observed by histological evaluation. Thus, the use of allogenic synovial MSCs did not appear to induce immunologic reactions in this osteochondral repair model, as was also shown in our previous porcine studies.[23,24]

In our preliminary study, we have created osteochondral defects of the same size (5 mm in diameter and 6 mm in depth) in the femoral groove and investigated their natural healing response out to 6 month postsurgery in rabbit model. The repair tissue in empty defect animals consistently showed delayed and insufficient subchondral bone repair with fibrous or fibro-cartilaginous tissue at 6 months postsurgery (Supplementary Fig. S1; Supplementary Data are available online at www.liebertpub.com/tea). Modified O'Driscoll histological scoring also showed significantly lower values either at the subchondral bone or cartilage areas (Supplementary Tables S1 and S2). Therefore, we have concluded that this osteochondral defect model is a critical size (incurable) defect model and thus, we have decided not to include the untreated defect group in the present study. We believe the lack of untreated defect group does not affect the major conclusions of the present study as the TEC-HA group fared much better than the HA group.

As for potential limitations of present studies, the origin of the cells involved in such time-course transitioning in osteochondral differentiation in the repair tissue in both groups could not be fully elucidated in the present study. A specific and stable labeling of the cells within the TEC will be required for such clarification. In addition, we did not use a large animal model such as pigs, goats, and sheep. An overgrowth of subchondral bone (thinning of cartilage) was observed at 6 months after surgery, and, therefore, it may be difficult to follow up for longer periods with this model. Similar phenomena have been previously reported in rabbit osteochondral defect models,[63] and it has been discussed that such phenomena might result from the acceleration of endochondral ossification or the degeneration of implanted MSCs.[64–66] Therefore, it may be necessary in the future to manipulate the *in vivo* differentiation processes in order to maintain a permanent cartilage phenotype by modulating endochondral ossification pathways.[67] Alternatively, the use of a larger animal model will be required for longer follow up postimplantation, which would further increase the clinical relevance of the findings.

Conclusion

In conclusion, the combined implant generated with an MSC-based TEC and a HA artificial bone significantly improved osteochondral repair as compared with the artificial bone alone. Moreover, time-course transitions in the development of osteochondral repair tissue were morphologically demonstrated to replace the original TEC after implantation. Specifically, the accelerated and improved repair of the subchndral bone, as well as good quality of the repair cartilage with secure tissue integration to the adjacent host tissue could warrant longer-term durability. Being scaffold free, the TEC contained no animal- or chemical-derived materials, and HA artificial bone has been widely used in clinical practice. Therefore, the TEC-HA combined construct could be considered a promising MSC-based bio-implant to repair osteochondral lesions with safety and cost effectiveness.

Acknowledgments

This study was supported by a grant from the New Energy and Industrial Technology Development Organization, Japan, and Grant in Aid for Scientific Research (B), Japan Society for the Promotion of Science, Japan.

Disclosure Statement

No competing financial interests exist.

References

1. Harris, E.D., Jr. The bone and joint decade: a catalyst for progress. Arthritis Rheum **44,** 1969, 2001.
2. Kon, E., Mandelbaum, B., Buda, R., Filardo, G., Delcogliano, M., Timoncini, A., *et al.* Platelet-rich plasma intra-articular injection versus hyaluronic acid viscosupplementation as treatments for cartilage pathology: from early degeneration to osteoarthritis. Arthroscopy **27,** 1490, 2011.
3. Filardo, G., Kon, E., Pereira Ruiz, M.T., Vaccaro, F., Guitaldi, R., Di Martino, A., *et al.* Platelet-rich plasma intra-articular injections for cartilage degeneration and osteoarthritis: single- versus double-spinning approach. Knee Surg Sports Traumatol Arthrosc **20,** 2082, 2012.
4. Bannuru, R.R., Natov, N.S., Obadan, I.E., Price, L.L., Schmid, C.H., and McAlindon, T.E. Therapeutic trajectory of hyaluronic acid versus corticosteroids in the treatment of knee osteoarthritis: a systematic review and meta-analysis. Arthritis Rheum **61,** 1704, 2009.
5. Kon, E., Delcogliano, M., Filardo, G., Busacca, M., Di Martino, A., and Marcacci, M. Novel nano-composite multilayered biomaterial for osteochondral regeneration: a pilot clinical trial. Am J Sports Med **39,** 1180, 2011.
6. Dhollander, A.A., Liekens, K., Almqvist, K.F., Verdonk, R., Lambrecht, S., Elewaut, D., *et al.* A pilot study of the use of an osteochondral scaffold plug for cartilage repair in the knee and how to deal with early clinical failures. Arthroscopy **28,** 225, 2012.
7. Gomoll, A.H., Madry, H., Knutsen, G., van Dijk, N., Seil, R., Brittberg, M., *et al.* The subchondral bone in articular cartilage repair: current problems in the surgical management. Knee Surg Sports Traumatol Arthrosc **18,** 434, 2010.
8. Minas, T., Gomoll, A.H., Rosenberger, R., Royce, R.O., and Bryant, T. Increased failure rate of autologous chondrocyte implantation after previous treatment with marrow stimulation techniques. Am J Sports Med **37,** 902, 2009.
9. Hung, C.T., Lima, E.G., Mauck, R.L., Takai, E., LeRoux, M.A., Lu, H.H., *et al.* Anatomically shaped osteochondral constructs for articular cartilage repair. J Biomech **36,** 1853, 2003.
10. Marquass, B., Somerson, J.S., Hepp, P., Aigner, T., Schwan, S., Bader, A., *et al.* A novel MSC-seeded triphasic construct for the repair of osteochondral defects. J Orthop Res **28,** 1586, 2010.
11. Oliveira, J.M., Rodrigues, M.T., Silva, S.S., Malafaya, P.B., Gomes, M.E., Viegas, C.A., *et al.* Novel hydroxyapatite/chitosan bilayered scaffold for osteochondral tissue-engineering applications: scaffold design and its performance when seeded with goat bone marrow stromal cells. Biomaterials **27,** 6123, 2006.
12. Sherwood, J.K., Riley, S.L., Palazzolo, R., Brown, S.C., Monkhouse, D.C., Coates, M., *et al.* A three-dimensional osteochondral composite scaffold for articular cartilage repair. Biomaterials **23,** 4739, 2002.
13. Ahn, J.H., Lee, T.H., Oh, J.S., Kim, S.Y., Kim, H.J., Park, I.K., *et al.* Novel hyaluronate-atelocollagen/beta-TCP-hydroxyapatite biphasic scaffold for the repair of osteochondral defects in rabbits. Tissue Eng Part A **15,** 2595, 2009.
14. Alhadlaq, A., and Mao, J.J. Tissue-engineered osteochondral constructs in the shape of an articular condyle. J Bone Joint Surg Am **87,** 936, 2005.
15. Gao, J., Dennis, J.E., Solchaga, L.A., Goldberg, V.M., and Caplan, A.I. Repair of osteochondral defect with tissue-engineered two-phase composite material of injectable calcium phosphate and hyaluronan sponge. Tissue Eng **8,** 827, 2002.
16. Kandel, R.A., Grynpas, M., Pilliar, R., Lee, J., Wang, J., Waldman, S., *et al.* Repair of osteochondral defects with biphasic cartilage-calcium polyphosphate constructs in a sheep model. Biomaterials **27,** 4120, 2006.
17. Chen, J., Chen, H., Li, P., Diao, H., Zhu, S., Dong, L., *et al.* Simultaneous regeneration of articular cartilage and subchondral bone *in vivo* using MSCs induced by a spatially controlled gene delivery system in bilayered integrated scaffolds. Biomaterials **32,** 4793, 2011.
18. Tamai, N., Myoui, A., Hirao, M., Kaito, T., Ochi, T., Tanaka, J., *et al.* A new biotechnology for articular cartilage repair: subchondral implantation of a composite of interconnected porous hydroxyapatite, synthetic polymer (PLA-PEG), and bone morphogenetic protein-2 (rhBMP-2). Osteoarthritis Cartilage **13,** 405, 2005.
19. Tamai, N., Myoui, A., Kudawara, I., Ueda, T., and Yoshikawa, H. Novel fully interconnected porous hydroxyapatite ceramic in surgical treatment of benign bone tumor. J Orthop Sci **15,** 560, 2010.
20. Shen, C., Ma, J., Chen, X.D., and Dai, L.Y. The use of beta-TCP in the surgical treatment of tibial plateau fractures. Knee Surg Sports Traumatol Arthrosc **17,** 1406, 2009.
21. Yamasaki, N., Hirao, M., Nanno, K., Sugiyasu, K., Tamai, N., Hashimoto, N., *et al.* A comparative assessment of synthetic ceramic bone substitutes with different composition and microstructure in rabbit femoral condyle model. J Biomed Mater Res B Appl Biomater **91,** 788, 2009.
22. Ando, W., Tateishi, K., Katakai, D., Hart, D.A., Higuchi, C., Nakata, K., *et al.* *In vitro* generation of a scaffold-free tissue-engineered construct (TEC) derived from human synovial mesenchymal stem cells: biological and mechanical properties and further chondrogenic potential. Tissue Eng Part A **14,** 2041, 2008.
23. Ando, W., Tateishi, K., Hart, D.A., Katakai, D., Tanaka, Y., Nakata, K., *et al.* Cartilage repair using an *in vitro* generated

scaffold-free tissue-engineered construct derived from porcine synovial mesenchymal stem cells. Biomaterials **28,** 5462, 2007.
24. Shimomura, K., Ando, W., Tateishi, K., Nansai, R., Fujie, H., Hart, D.A., *et al.* The influence of skeletal maturity on allogenic synovial mesenchymal stem cell-based repair of cartilage in a large animal model. Biomaterials **31,** 8004, 2010.
25. Nansai, R., Suzuki, T., Shimomura, K., Ando, W., Nakamura, N., and Fujie, H. Surface morphology and stiffness of cartilage-like tissue repaired with a scaffold-free tissue engineered construct. J Biomech Sci Eng **6,** 40, 2011.
26. Tateishi, K., Higuchi, C., Ando, W., Nakata, K., Hashimoto, J., Hart, D.A., *et al.* The immunosuppressant FK506 promotes development of the chondrogenic phenotype in human synovial stromal cells via modulation of the Smad signaling pathway. Osteoarthritis Cartilage **15,** 709, 2007.
27. O'Driscoll, S.W., Keeley, F.W., and Salter, R.B. Durability of regenerated articular cartilage produced by free autogenous periosteal grafts in major full-thickness defects in joint surfaces under the influence of continuous passive motion. A follow-up report at one year. J Bone Joint Surg Am **70,** 595, 1988.
28. Mrosek, E.H., Schagemann, J.C., Chung, H.W., Fitzsimmons, J.S., Yaszemski, M.J., Mardones, R.M., *et al.* Porous tantalum and poly-epsilon-caprolactone biocomposites for osteochondral defect repair: preliminary studies in rabbits. J Orthop Res **28,** 141, 2010.
29. Olivos-Meza, A., Fitzsimmons, J.S., Casper, M.E., Chen, Q., An, K.N., Ruesink, T.J., *et al.* Pretreatment of periosteum with TGF-beta1 *in situ* enhances the quality of osteochondral tissue regenerated from transplanted periosteal grafts in adult rabbits. Osteoarthritis Cartilage **18,** 1183, 2010.
30. Salzmann, G.M., Paul, J., Bauer, J.S., Woertler, K., Sauerschnig, M., Landwehr, S., *et al.* T2 assessment and clinical outcome following autologous matrix-assisted chondrocyte and osteochondral autograft transplantation. Osteoarthritis Cartilage **17,** 1576, 2009.
31. Basad, E., Ishaque, B., Bachmann, G., Sturz, H., and Steinmeyer, J. Matrix-induced autologous chondrocyte implantation versus microfracture in the treatment of cartilage defects of the knee: a 2-year randomised study. Knee Surg Sports Traumatol Arthrosc **18,** 519, 2010.
32. Ferruzzi, A., Buda, R., Faldini, C., Vannini, F., Di Caprio, F., Luciani, D., *et al.* Autologous chondrocyte implantation in the knee joint: open compared with arthroscopic technique. Comparison at a minimum follow-up of five years. J Bone Joint Surg Am **90 Suppl 4,** 90, 2008.
33. Kon, E., Filardo, G., Condello, V., Collarile, M., Di Martino, A., Zorzi, C., *et al.* Second-generation autologous chondrocyte implantation: results in patients older than 40 years. Am J Sports Med **39,** 1668, 2011.
34. Stanish, W.D., McCormack, R., Forriol, F., Mohtadi, N., Pelet, S., Desnoyers, J., *et al.* Novel scaffold-based BST-CarGel treatment results in superior cartilage repair compared with microfracture in a randomized controlled trial. J Bone Joint Surg Am **95,** 1640, 2013.
35. Crawford, D.C., DeBerardino, T.M., and Williams, R.J., 3rd. NeoCart, an autologous cartilage tissue implant, compared with microfracture for treatment of distal femoral cartilage lesions: an FDA phase-II prospective, randomized clinical trial after two years. J Bone Joint Surg Am **94,** 979, 2012.
36. Curl, W.W., Krome, J., Gordon, E.S., Rushing, J., Smith, B.P., and Poehling, G.G. Cartilage injuries: a review of 31,516 knee arthroscopies. Arthroscopy **13,** 456, 1997.
37. Hjelle, K., Solheim, E., Strand, T., Muri, R., and Brittberg, M. Articular cartilage defects in 1,000 knee arthroscopies. Arthroscopy **18,** 730, 2002.
38. Aroen, A., Loken, S., Heir, S., Alvik, E., Ekeland, A., Granlund, O.G., *et al.* Articular cartilage lesions in 993 consecutive knee arthroscopies. Am J Sports Med **32,** 211, 2004.
39. Zhang, W., Moskowitz, R.W., Nuki, G., Abramson, S., Altman, R.D., Arden, N., *et al.* OARSI recommendations for the management of hip and knee osteoarthritis, Part II: OARSI evidence-based, expert consensus guidelines. Osteoarthritis Cartilage **16,** 137, 2008.
40. Dawson, J., Linsell, L., Zondervan, K., Rose, P., Randall, T., Carr, A., *et al.* Epidemiology of hip and knee pain and its impact on overall health status in older adults. Rheumatology (Oxford) **43,** 497, 2004.
41. Peat, G., McCarney, R., and Croft, P. Knee pain and osteoarthritis in older adults: a review of community burden and current use of primary health care. Ann Rheum Dis **60,** 91, 2001.
42. Zhang, S., Chen, L., Jiang, Y., Cai, Y., Xu, G., Tong, T., *et al.* Bi-layer collagen/microporous electrospun nanofiber scaffold improves the osteochondral regeneration. Acta Biomater **9,** 7236, 2013.
43. Schleicher, I., Lips, K.S., Sommer, U., Schappat, I., Martin, A.P., Szalay, G., *et al.* Biphasic scaffolds for repair of deep osteochondral defects in a sheep model. J Surg Res **183,** 184, 2013.
44. Kon, E., Filardo, G., Robinson, D., Eisman, J.A., Levy, A., Zaslav, K., *et al.* Osteochondral regeneration using a novel aragonite-hyaluronate bi-phasic scaffold in a goat model. Knee Surg Sports Traumatol Arthrosc 2013. DOI: 10.1007/s00167-013-2467-2
45. Marmotti, A., Bruzzone, M., Bonasia, D.E., Castoldi, F., Von Degerfeld, M.M., Bignardi, C., *et al.* Autologous cartilage fragments in a composite scaffold for one stage osteochondral repair in a goat model. Eur Cell Mater **26,** 15, discussion −2, 2013.
46. Miot, S., Brehm, W., Dickinson, S., Sims, T., Wixmerten, A., Longinotti, C., *et al.* Influence of *in vitro* maturation of engineered cartilage on the outcome of osteochondral repair in a goat model. Eur Cell Mater **23,** 222, 2012.
47. Filardo, G., Kon, E., Di Martino, A., Busacca, M., Altadonna, G., and Marcacci, M. Treatment of knee osteochondritis dissecans with a cell-free biomimetic osteochondral scaffold: clinical and imaging evaluation at 2-year follow-up. Am J Sports Med **41,** 1786, 2013.
48. Kon, E., Filardo, G., Di Martino, A., Busacca, M., Moio, A., Perdisa, F., *et al.* Clinical results and MRI evolution of a nano-composite multilayered biomaterial for osteochondral regeneration at 5 years. Am J Sports Med **42,** 158, 2014.
49. Delcogliano, M., de Caro, F., Scaravella, E., Ziveri, G., De Biase, C.F., Marotta, D., *et al.* Use of innovative biomimetic scaffold in the treatment for large osteochondral lesions of the knee. Knee Surg Sports Traumatol Arthrosc 2013. [Epub ahead of print] DOI: 10.1007/s00167-013-2717-3
50. Nooeaid, P., Salih, V., Beier, J.P., and Boccaccini, A.R. Osteochondral tissue engineering: scaffolds, stem cells and applications. J Cell Mol Med **16,** 2247, 2012.
51. Deie, M., Ochi, M., Adachi, N., Nishimori, M., and Yokota, K. Artificial bone grafting [calcium hydroxyapatite ceramic

with an interconnected porous structure (IP-CHA)] and core decompression for spontaneous osteonecrosis of the femoral condyle in the knee. Knee Surg Sports Traumatol Arthrosc **16,** 753, 2008.
52. Kuriyama, K., Hashimoto, J., Murase, T., Fujii, M., Nampei, A., Hirao, M., *et al.* Treatment of juxta-articular intraosseous cystic lesions in rheumatoid arthritis patients with interconnected porous calcium hydroxyapatite ceramic. Mod Rheumatol **19,** 180, 2009.
53. Miot, S., Scandiucci de Freitas, P., Wirz, D., Daniels, A.U., Sims, T.J., Hollander, A.P., *et al.* Cartilage tissue engineering by expanded goat articular chondrocytes. J Orthop Res **24,** 1078, 2006.
54. Poole, C.A., Matsuoka, A., and Schofield, J.R. Chondrons from articular cartilage. III. Morphologic changes in the cellular microenvironment of chondrons isolated from osteoarthritic cartilage. Arthritis Rheum **34,** 22, 1991.
55. Muldrew, K., Chung, M., Novak, K., Schachar, N.S., Zernicke, R.F., McGann, L.E., *et al.* Evidence of chondrocyte repopulation in adult ovine articular cartilage following cryoinjury and long-term transplantation. Osteoarthritis Cartilage **9,** 432, 2001.
56. Quintavalla, J., Kumar, C., Daouti, S., Slosberg, E., and Uziel-Fusi, S. Chondrocyte cluster formation in agarose cultures as a functional assay to identify genes expressed in osteoarthritis. J Cell Physiol **204,** 560, 2005.
57. Khan, I.M., Palmer, E.A., and Archer, C.W. Fibroblast growth factor-2 induced chondrocyte cluster formation in experimentally wounded articular cartilage is blocked by soluble Jagged-1. Osteoarthritis Cartilage **18,** 208, 2010.
58. McCormack, T., and Mansour, J.M. Reduction in tensile strength of cartilage precedes surface damage under repeated compressive loading *in vitro*. J Biomech **31,** 55, 1998.
59. Roemhildt, M.L., Beynnon, B.D., Gauthier, A.E., Gardner-Morse, M., Ertem, F., and Badger, G.J. Chronic *in vivo* load alteration induces degenerative changes in the rat tibiofemoral joint. Osteoarthritis Cartilage **21,** 346, 2013.
60. Hosseini, S.M., Veldink, M.B., Ito, K., and van Donkelaar, C.C. Is collagen fiber damage the cause of early softening in articular cartilage? Osteoarthritis Cartilage **21,** 136, 2013.
61. Ryan, J.M., Barry, F.P., Murphy, J.M., and Mahon, B.P. Mesenchymal stem cells avoid allogeneic rejection. J Inflamm (Lond) **2,** 8, 2005.
62. Griffin, M.D., Ritter, T., and Mahon, B.P. Immunological aspects of allogeneic mesenchymal stem cell therapies. Hum Gene Ther **21,** 1641, 2010.
63. Wakitani, S., Goto, T., Pineda, S.J., Young, R.G., Mansour, J.M., Caplan, A.I., *et al.* Mesenchymal cell-based repair of large, full-thickness defects of articular cartilage. J Bone Joint Surg Am **76,** 579, 1994.
64. Chen, H., Chevrier, A., Hoemann, C.D., Sun, J., Ouyang, W., and Buschmann, M.D. Characterization of subchondral bone repair for marrow-stimulated chondral defects and its relationship to articular cartilage resurfacing. Am J Sports Med **39,** 1731, 2011.
65. Bedi, A., Feeley, B.T., and Williams, R.J., 3rd. Management of articular cartilage defects of the knee. J Bone Joint Surg Am **92,** 994, 2010.
66. Vasara, A.I., Hyttinen, M.M., Lammi, M.J., Lammi, P.E., Langsjo, T.K., Lindahl, A., *et al.* Subchondral bone reaction associated with chondral defect and attempted cartilage repair in goats. Calcif Tissue Int **74,** 107, 2004.
67. Liu, G., Kawaguchi, H., Ogasawara, T., Asawa, Y., Kishimoto, J., Takahashi, T., *et al.* Optimal combination of soluble factors for tissue engineering of permanent cartilage from cultured human chondrocytes. J Biol Chem **282,** 20407, 2007.

Address correspondence to:
Norimasa Nakamura, MD, PhD
Institute for Medical Science in Sports
Osaka Health Science University
1-9-27, Tenma, Kita-ku
Osaka 530-0043
Japan

E-mail: norimasa.nakamura@ohsu.ac.jp

Received: July 6, 2013
Accepted: February 5, 2014
Online Publication Date: March 19, 2014

Cytotherapy, 2014; 16: 776–788

International Society for Cellular Therapy ISCT®

Clonal analysis of synovial fluid stem cells to characterize and identify stable mesenchymal stromal cell/mesenchymal progenitor cell phenotypes in a porcine model: a cell source with enhanced commitment to the chondrogenic lineage

WATARU ANDO[1,2,*], JOSH J. KUTCHER[1,*], ROMAN KRAWETZ[1], ARINDOM SEN[1,3], NORIMASA NAKAMURA[2], CYRIL B. FRANK[1] & DAVID A. HART[1]

[1]McCaig Institute for Bone and Joint Health, University of Calgary, Calgary, Alberta, Canada, [2]Department of Orthopedic Surgery, Osaka University, Graduate School of Medicine, Suita, Osaka, Japan, and [3]Pharmaceutical Production Research Facility, Schulich School of Engineering, University of Calgary, Calgary, Alberta, Canada

Abstract

Background aims. Previous studies have demonstrated that porcine synovial membrane stem cells can adhere to a cartilage defect *in vivo* through the use of a tissue-engineered construct approach. To optimize this model, we wanted to compare effectiveness of tissue sources to determine whether porcine synovial fluid, synovial membrane, bone marrow and skin sources replicate our understanding of synovial fluid mesenchymal stromal cells or mesenchymal progenitor cells from humans both at the population level and the single-cell level. Synovial fluid clones were subsequently isolated and characterized to identify cells with a highly characterized optimal phenotype. *Methods.* The chondrogenic, osteogenic and adipogenic potentials were assessed *in vitro* for skin, bone marrow, adipose, synovial fluid and synovial membrane–derived stem cells. Synovial fluid cells then underwent limiting dilution analysis to isolate single clonal populations. These clonal populations were assessed for proliferative and differentiation potential by use of standardized protocols. *Results.* Porcine-derived cells demonstrated the same relationship between cell sources as that demonstrated previously for humans, suggesting that the pig may be an ideal preclinical animal model. Synovial fluid cells demonstrated the highest chondrogenic potential that was further characterized, demonstrating the existence of a unique clonal phenotype with enhanced chondrogenic potential. *Conclusions.* Porcine stem cells demonstrate characteristics similar to those in human-derived mesenchymal stromal cells from the same sources. Synovial fluid–derived stem cells contain an inherent phenotype that may be optimal for cartilage repair. This must be more fully investigated for future use in the *in vivo* tissue-engineered construct approach in this physiologically relevant preclinical porcine model.

Key Words: *chondrogenesis, mesenchymal stromal cells, porcine, synovial fluid, synovium*

Introduction

Articular cartilage damage is a common clinical problem that has garnered extensive research attention during the past decade, particularly though stem cell modalities. Chondrocytes, which are a distinct and unique cell type located within cartilage, exhibit a limited repair capacity, meaning that damaged cartilage will not spontaneously regenerate. Advanced degradation of joints routinely leads to replacement by artificial joints. Whereas these biomedical devices have shown efficacy in restoring function, they are plagued by a number of side effects, are not durable for extended periods of time and are not as effective as an actual joint. Cell-based therapies are now being examined as a means to regenerate cartilage. Advances in tissue engineering, led by research into cell biology and biomaterials, are enabling regenerative medicine to emerge as a potential alternative to artificial joints. Cell therapies may provide a novel therapeutic approach for controlling progression of diseases that alter chondrocytic function as well as to promote cellular regeneration. Autologous chondrocyte implantation is a fairly recent cell therapy that involves the isolation chondrocytes from a cartilage biopsy taken from a healthy and minor load-bearing area of the afflicted

*These authors contributed equally to this work.
Correspondence: **Josh Kutcher**, MSc, McCaig Institute for Bone and Joint Health, 306-8210 111 street, Edmonton, Alberta, Canada, T6G2C7. E-mail: jjkutche@gmail.com

(Received 21 June 2013; accepted 10 December 2013)

ISSN 1465-3249
http://dx.doi.org/10.1016/j.jcyt.2013.12.003

joint surface (1). This procedure has undergone clinical trials demonstrating some long-term efficacy (2). However, in some patients, the repair tissue is a fibrocartilage (3) rather than hyaline-like, which may be attributable to the fact that culture expansion of chondrocytes may lead to dedifferentiation or an unstable phenotype and inevitably a loss of chondrogenic potential *in vivo* (4). In addition to this limitation, the chondrocyte biopsy itself may result in further joint damage and so the need has arisen for a new source of cells that may be used therapeutically, ultimately in a minimally invasive fashion and with a stable phenotype. Mesenchymal stromal cells (MSCs) are promising because they are highly proliferative, undifferentiated cells with the potential to expand extensively and differentiate into several lineages (5). Currently, the outcomes of cell therapies are inadequate; one of the primary complications is caused by difficulties in maintaining a stable chondrocytic phenotype. Autologous cell therapies with the use of highly characterized clonal MSCs or mesenchymal progenitor cells (MPCs) may be a viable alternative because cells can be selected with optimized properties for the specific application of interest. It is known that synovial fluid (SF) MSCs/MPCs from injured or diseased joints may not be ideal because they can be compromised by an inflammatory microenvironment (6,7). It is well documented that human synovium contains an inherent MSC/MPC population with an enhanced propensity for chondrogenesis (8). Recently, we demonstrated that porcine synovial cells exhibit enhanced chondrogenic potential and can repair cartilage *in vivo*, (9) similar to that demonstrated in human synovium-derived stem cells (8). We have also demonstrated this previously in a porcine model (10) as well as with human MSCs (11). However, the cell populations used in these studies probably were a mixed heterogeneous population because they were derived from multiple clones, and, as such, phenotypic stability may be questionable because of the presence of heterogeneity between subsets during culture expansion (12). SF contains an inherent stem cell population (13) that can be accessed with minimally invasive methods and requires less processing than synovium, reducing the risk of contamination. In particular, the use of collagenase has been linked to potential bovine spongiform encephalopathy contamination. Because of the ease of isolation and less need for extensive processing, SF-derived cells may be an ideal candidate cell source for clinical applications; however, further examination is needed. Our initial studies indicate that SF may be able to regenerate cartilage more efficiently than other tissue types. Because of the heterogeneity that is present in stem cell populations, examining the single clonal population may also be a more effective method of repairing cartilage by increasing the consistency and predictability of these clonal cells. Therefore, the objectives of the current studies were to both confirm that porcine SF is an effective cell source for chondrogenesis and to establish the proliferative and differentiation characteristics of individual clonal populations, which could ultimately be used to select highly characterized cells with a defined and optimal phenotype. This would provide an opportunity to optimize the tissue-engineered construct (TEC) approach in a porcine model before clinical investigation.

Methods

Collection and isolation of cells from porcine knees

The animal protocols were approved by the institutional ethics committee at the University of Calgary Health Sciences Centre. SF was obtained from the hind legs of three female juvenile Yorkshire pigs between 3–4 months old and weighing 25–30 kg (Table I). After euthanasia, a medial parapatellar incision was made and the SF was aspirated with the use of a 23-gauge needle before opening the knee capsule. After ensuring complete aspiration of SF, 10 mL of sterile pyrogen-free phosphate-buffered saline (PBS) (Invitrogen, Carlsbad, CA, USA) was injected to expand the knee joint space, and this fluid was then re-aspirated. The cell isolation protocol for synovial membranes (SM) was identical to that described previously (10). Briefly, SM specimens were obtained aseptically from the knee of the same pig after collecting SF, and the tissue was then minced meticulously. The minced tissue was digested with 0.2% collagenase (Worthington Biochemical Corp, Lakewood, NJ, USA). After removal of full-thickness skin, adipose tissue cells were obtained from the subcutaneous tissues, and the same procedure was followed as that for the cell isolation of SM. Bone marrow (BM) was obtained from the femurs of each pig by aspiration. Freshly isolated cells were diluted 1:4 with PBS and obtained by centrifugation. All cells were then resuspended in basic culture growth media containing high-glucose Dulbecco's modified Eagle's medium (DMEM; Invitrogen) supplemented with 10% fetal bovine serum (Invitrogen) and 1% antibiotic/antimycotic (Invitrogen Canada Inc) and were then plated in T-25 cell culture flasks (BD Bioscience, San Jose, CA, USA). Non-adherent cells were removed by changing the media. Cells were then

Table I. Characteristics of porcine subjects.

Subject	Age, months	Sex	Weight, kg	Passage
A	3	Female	26.2	3
B	3	Female	29.3	3
C	4	Female	27.8	3

counted with the use of trypan blue (Sigma Aldrich, St. Louis, MO, USA) to assess cell viability and subsequently either underwent culture expansion in growth media or were used for limiting dilution to generate single-cell–derived clonal populations.

Cell expansion and cryopreservation

For expansion, cells were cultured in monolayers in a humidified atmosphere of 5% CO_2 at 37°C. The growth media was changed every 3 days until 80% confluent for the duration of the expansion process, after which the cells were rinsed with PBS and harvested with 0.25% trypsin-EDTA (Invitrogen). Cells were counted with the use of a hemocytometer and plated at a density of 3000/cm^2 and continually passaged until 80% confluent. At passage 3, aliquots of trypsin-released cells in DMEM with 40% fetal bovine serum and 10% DMSO Invitrogen were cryopreserved in liquid nitrogen.

Cell cloning of SF-derived progenitor cells

Limiting dilution was used to establish clonal populations (13). First-passage SF cells were suspended in growth media and plated at a density of 0.5 cells/well in 96-well, flat-bottomed culture plates (BD Bioscience). Cell populations arising from a single cell were identified by light microscopy and subsequently expanded on confluence. Eight expandable clones were obtained from each of the three pigs, and six of eight were randomly selected for expansion and characterization (18 total clones), whereas the remaining six clones were subjected to cryopreservation. These populations are referred to as clonal populations.

Growth kinetics

Cells were consistently plated on confluence at a density of 3000 cells/cm^2. Trypan blue staining and a hemocytometer were used to assess that cell viability at each passage was >90%. The growth rate of each clone is expressed as population doubling (PD) time and displayed against culture duration for each cell to undergo 30 PD times.

In vitro chondrogenesis assay

Each of the six clonal populations and six mixed populations from each of the three pigs (n = 18) were expanded in a monolayer with the use of four T-75 flasks each to provide a total of approximately 3 million cells per clone estimated to be required to perform all experiments. SF-derived cells were released by trypsin treatment and viable cells were counted with the use of trypan blue. Micro-suspension cultures were obtained by resuspending the cells at a density of 2.0×10^7 viable cells per milliliter and pipetting droplets of cell suspension into individual flat-bottomed wells (14). Samples to be used for RNA extraction and subsequent quantitative polymerase chain reaction (qPCR) analysis were cultured in 24-well plates with the use of 20-μL droplets, which is the equivalent of roughly 400,000 cells per well, and was performed in triplicate. Samples to undergo specific molecular staining and analyzed with light microscopy were cultured in 48-well plates with 10-μL droplets, which contained approximately 200,000 cells. After cells were allowed to attach (2–4 h), basic growth medium was added, and this was designated day 0.

On day 1, the culture medium was replaced with DMEM supplemented with insulin-transferrin-selenium +1 (GIBCO), 0.2 mmol/L of ascorbic acid-2–phosphate (Sigma-Aldrich), 10^{-7} mol/L dexamethasone (Sigma-Aldrich), 100 ng/mL recombinant human bone morphogenic protein (Peprotech Inc, Rocky Hill, NJ, USA) and 10 ng/mL recombinant human transforming growth factor β1 (Peptrotech) dissolved in 3 mmol/L acetic acid, containing 1 mg/mL of bovine serum albumin (Sigma-Aldrich). Identical amounts of acetic acid and bovine serum albumin were used for the control groups with growth medium. The chondrogenic medium and control medium were replaced every 3 days for a total of 21 days.

On day 21, cells in 48-well plates were rinsed twice with PBS and fixed with 4% paraformaldehyde (PFA; Fischer, Ottawa, ON, CA) for 30 min at room temperature. After rinsing with PBS three times, cells were covered with 0.5% alcian blue 8 GS (Sigma-Aldrich) (pH 2.5 in 3% acetic acid) and left overnight. This was followed by rinsing with acetic acid and then PBS and was subsequently examined with the use of light microscopy for cartilage-specific proteoglycans. Cells in 24-well plates were extracted with, and then stored in, TRIzol reagent at −80°C for subsequent molecular analysis.

In vitro osteogenesis assay

SF-derived clonal and mixed cell populations were plated at 3000 cells per cm^2 in 24-and 48-well flat-bottomed culture plates (day 0). The following day, fresh growth medium supplemented with 100 nmol/L dexamethasone, 10 mmol/L β-glycerophosphate (Sigma Aldrich) and 50 μmol/L ascorbic acid-2-phosphate was provided, and DMEM was added to the control wells. Medium was changed every 3 days, and, similar to the chondrogenic assay, cells in the 24-well plates were collected with TRIzol for subsequent molecular analysis.

To determine alkaline phosphatase activity, cells were fixed with 4% PFA for 1–2 min (to prevent inactivation of alkaline phosphatase) and assayed

with the use of a commercially available kit (Millipore, Billerica, MA, USA; SCR004). To stain for calcium deposits, cells were rinsed with PBS and covered with alizarin red S (Sigma-Aldrich) (2% aqueous solution). Cultures were then washed thoroughly with distilled water.

In vitro adipogenesis assay

SF-derived cloned cells and mixed cell populations were plated at a density of 1000 cells per cm^2 in the same fashion as the osteogenic assays. On day 1, adipogenic induction medium consisting of 1 μmol/L dexamethasone, 0.5 mmol/L 3-isobutyl-1-methylxanthine, 0.1 mmol/L indomethacin and 10 μg/mL insulin (all from Sigma) was used. After each 72-h period, the medium was changed to adipogenic maintenance medium (growth medium with 10 μg/mL insulin) for 24 h before being changed back to induction medium. This pattern was followed for 21 days, after which 24-well plates were cryopreserved with TRIzol reagent for further molecular analysis.

To detect lipid vacuoles, cells were rinsed with PBS twice and fixed with 4% PFA for 30 min. After rinsing with sterile water and 60% isopropanol, cells were covered with oil red O solution (0.1% oil red O (Sigma) in 60% isopropanol) for 5 min and were then rinsed with distilled water.

Reverse transcription–polymerase chain reaction and real-time RT-qPCR analysis

Total RNA was isolated from cells before differentiation and from cells cultured in chondrogenic medium with the use of the TRIspin method (15). One microgram of total RNA from each sample was initially reverse-transcribed with random RT primers with the use of an Omniscript RT kit (Qiagen, Hilden, Germany). Type II collagen and osteocalcin expression was assessed for determining chondrogenesis by semi-quantitative reverse transcription–PCR (RT-PCR), with the use of porcine-specific PCR primers as described in Table II. The protocol described previously (16,17) was used throughout. Amplicons were separated on a 2% agarose gel followed by staining with ethidium bromide and band detection with the use of a GelDoc system (Bio-Rad, Hercules, CA, USA).

qRT-PCR was performed to determine messenger RNA (mRNA) levels for specific molecules as described in Table II. The molecules chosen for assessment were a highly relevant subset reported to be associated with mesenchymal specific lineage (*Sox 9*–chondrogenic, *PPAR-γ*–adipogenic, *cbfa1*–osteogenic) (18) as well as specific osteogenic markers (VCAM and type I collagen) (19,20) in cells before the differentiation protocols. RT-qPCR was performed with the use of Bio-Rad iQ SYBR Green Supermix (Bio-Rad), as previously described (19). PCR primers and the annealing temperatures are listed in Table II. Amplification and detection were performed with the use of an iCycler Thermal Cycler (Bio-Rad). The levels for 18S were used as an endogenous standard for normalization. The quantification of the relative fold change between samples was analyzed with the use of iCycler iQ Optical System Software, version 3.0a (Bio-Rad). Each of the complementary DNA preparations was tested in duplicate. The standard curve method was used to quantify the relative change fold between samples (20). The correlation coefficient of each standard curve was approximately 0.99.

Statistical analysis

The results are presented as mean ± standard deviation. Measurements of cross-sectional area, GAG/

Table II. Primers used for quantitative real-time PCR analysis.

Gene	Gene ID	Primer sequence	Tm (°C)	Size (bp)	Reference
18S (human)	X03205	F; TGGTCGCTCGCTCCTCTCC R; CGCCTGCTGCCTTCCTTGG	65	360	Original
Col2a1 (bovine)	X02420	F; GAGCAGCAAGAGCAAGGACAAG R; GTAGGTGATGTTCTGAGAGCCCTC	53	163	Original
OCN	AW346755	F; TCAACCCCGACTGCGACGAG R; TTGGAGCAGCTGGGATGATGG	61	204	Zou, 2008[20]
Sox9	NM213843	F; CCGGTGCGCGTCAAC R; TGCAGGTGCGGGTACTGAT	59	119	Zou, 2008[20]
Cbfa1	BE234439	F; GAGGAACCGTTTCAGCTTACTG R; CGTTAACCAATGGCACGAG	59	167	Zou, 2008[20]
PPAR-γ	AF103946	F; GCGCCCTGGCAAAGCACT R; TCCACGGAGCGAAACTGACAC	63	238	Zou, 2008[20]
VCAM	U08351	F; CGAAAATCCTCTGGAGCAAG R; GACAGTGTCCCCTTCCTTGA	61	233	Original
Col1a1	AF201723	F;CCAAGAGGAGGGCCAAGAAGAAGG R; GGGGCAGACGGGGCAGCACTC	63	232	Zou, 2008[20]

protein, Ca and the elution of oil red O were analyzed by means of the Mann-Whitney *U* test. Linear regression analysis was used to explore the correlation between gene expression levels and differentiation markers. We used STATVIEW version 5.5 software (SAS Institute, Cary, NC, USA) to perform statistics, and significance was set at $P < 0.05$.

Ethics

The animal protocols were approved by the institutional ethics committee at the University of Calgary Health Sciences Centre.

Results

Expansion of SF MSC/MPC cells isolated without collagenase digestion is similar to cells from other sources

Four days after being isolated from their primary sources, larger numbers of cells were initially observed in cultures derived from the SM and skin (SK) samples with collagenase digestion than from SF and BM obtained without collagenase treatment. In all cases, the cell morphology was variable and contained both spindle-shaped cells and round cells. By day 10 after isolation, all cultures exhibited a sub-confluent adherent cell monolayer composed primarily of spindle-shaped cells (Figure 1). Surface markers CD29 and CD90 were positive, and CD14 and CD45 were negative in SF-derived cells, and these patterns were very similar to those obtained with SM, BM and SK cells (data not shown). Cells were then re-plated at 1×10^4 cells/cm^2 every 14 days.

Comparison of chondrogenic differentiation potential of cell populations from different sources

Cell pellets were cultured in basic culture medium (basal) or chondrogenic medium. All sources of cell pellets cultured in chondrogenic medium were larger than those cultured in basic culture medium (Figure 2A). The ratio between the cross-sectional areas of chondrogenic cell pellets and basal cell pellets revealed that SF cell pellets (3.05 ± 0.87) had similar chondrogenic potential compared with the SM cell pellets (2.49 ± 0.10) and significantly greater chondrogenic potential than the BM (1.68 ± 0.24) and SK (1.99 ± 0.29) cell pellets when cultured in chondrogenic medium (Figure 2B). The ratio between GAG expression of chondrogenic cell pellets and basal cell pellets revealed that SF cell pellets (12.4 ± 5.05) had similar chondrogenic potential compared with the SM cell pellets (8.61 ± 8.40) and significantly greater than the BM (2.27 ± 1.19) and SK (3.74 ± 3.19) cell pellets (Figure 2C). RT-PCR confirmed the mRNA expression levels for type II collagen in the cells from each source cultured in chondrogenic medium. Moreover, the mRNA levels for type II collagen in SM and SF cells cultured in chondrogenic medium were significantly higher than those in BM and SK cells ($P < 0.05$) (Figure 2D).

Comparison of osteogenic differentiation potential of cells from different sources

Alizarin red staining showed that cells from all sources were intensely stained with alizarin red when cultured in osteogenic induction medium, whereas cells cultured in basic culture medium were not stained (Figure 3A). BM cells were the most intensely stained. Calcium deposition by BM cells cultured in osteogenic induction medium (57.4 ± 3.60 μg/mL) was also significantly greater than that of SM (37.35 ± 8.35 μg/mL), SF (30.9 ± 7.81 μg/mL) and SK cells (38.8 ± 11.0 μg/mL) ($P < 0.001$) (Figure 3B). RT-PCR confirmed the upregulation of mRNA expression for osteocalcin (OCN) in the cells from each source cultured in osteogenic medium compared with those cultured in the basic culture medium (Figure 3C).

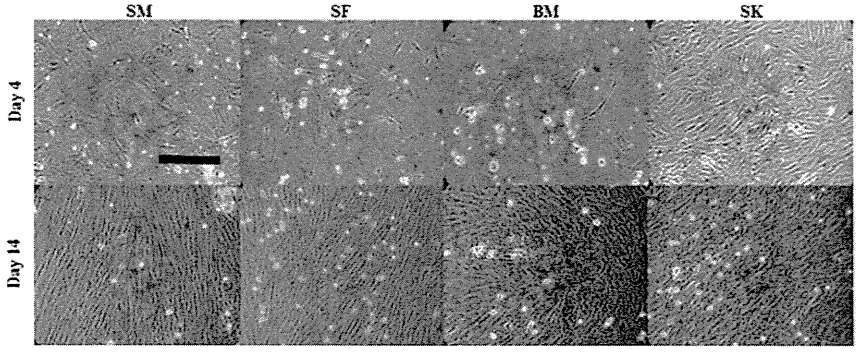

Figure 1. Cell morphology. Photomicrographs show the morphology of cells derived from SM and SK with collagenase digestion or SF and BM without collagenase digestion at day 4 and day 14 after isolation. Bar = 200 μm.

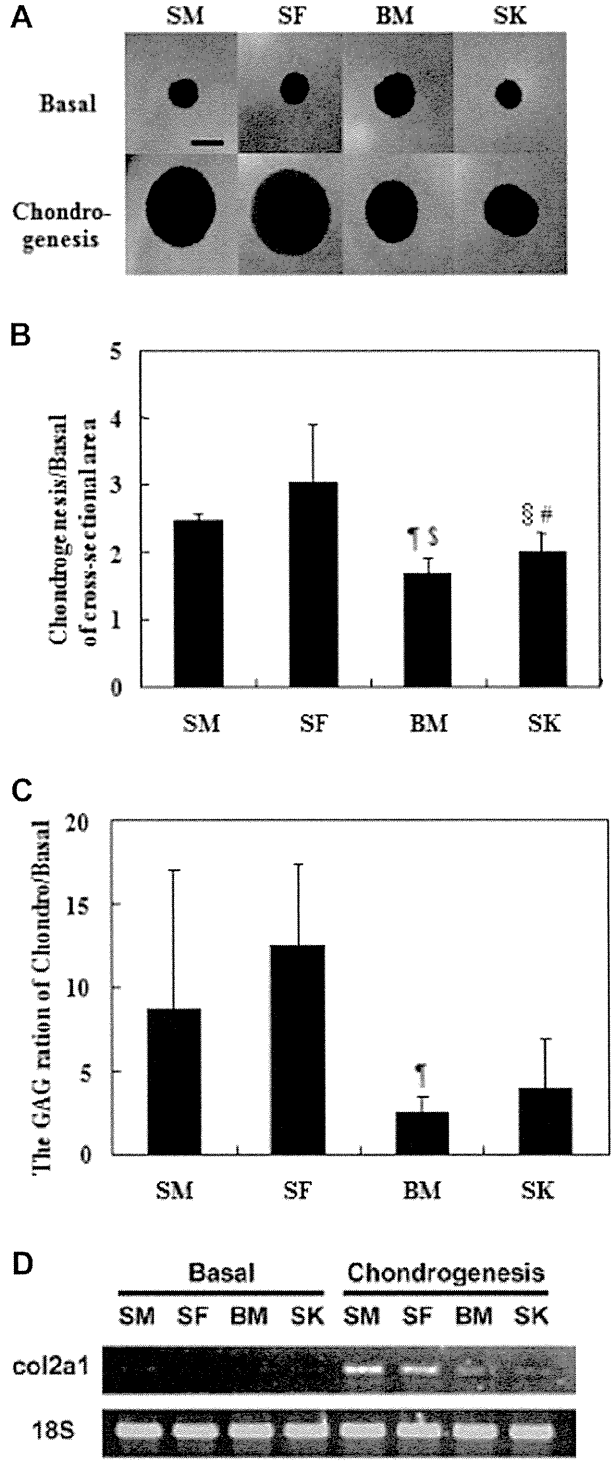

Figure 2. Comparison of the chondrogenic differentiation potential of cells from different sources. (A) Photographs of cell pellet–generated cells derived from SM, SF, BM and SK cultured in basic culture medium (basal) or chondrogenic induction medium (chondrogenesis). Size of all cell pellets increased when cultured in chondrogenic medium. Bar = 500 μm. (B) Ratio of cross-sectional areas for pellets derived from SM, SF, BM and SK in chondrogenic medium to pellets in basal medium (n = 4, $^{¶,§}P < 0.05$) compared with SM cells ($^{\$,\#}P < 0.05$) compared with SF cells. (C) Amount of glycosaminoglycan content in pellets generated from SM, SF, BM and SK cells in each animal (n = 4, $^{¶}P < 0.05$) compared with SF cells. (D) Induction of Col2a1 during chondrogenesis in the MSC from the four tissue sources.

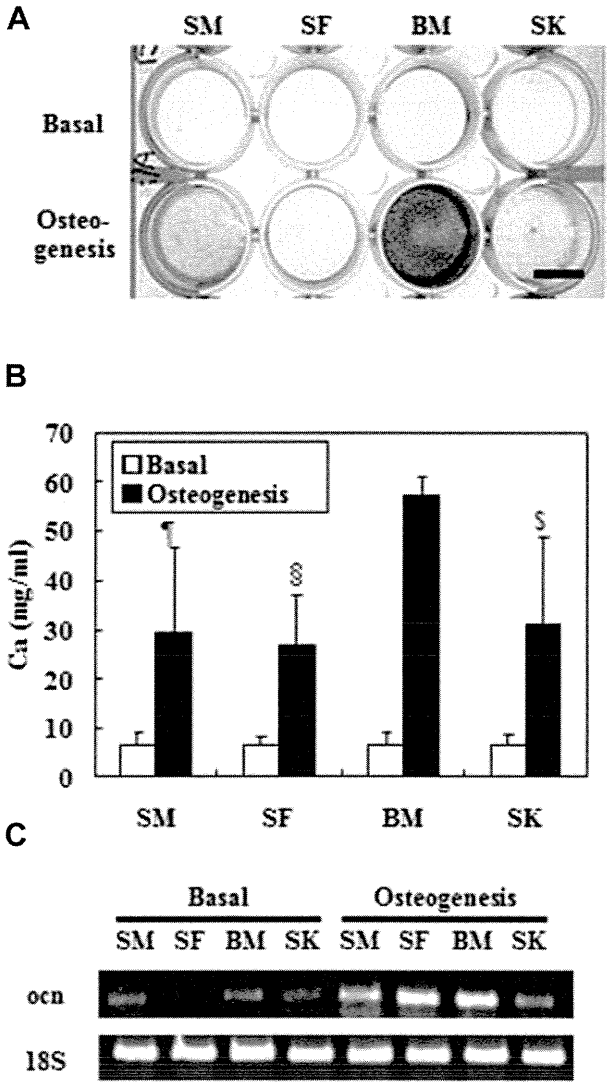

Figure 3. Comparison of the osteogenic differentiation potential of cells from different sources. (A) Alizarin red staining of cells from SM, SF, BM and SK cultured in basic culture medium (basal) or osteogenic induction medium (osteogenesis). Bar = 1 mm. (B) Calcium content of SM-, SF-, BM- and SK-derived cells in basic culture medium or osteogenic medium (n = 4, $^{¶,§,\$}P < 0.05$) compared with BM-derived cells. (C) Semi-quantitative RT-PCR analysis of cells from each tissue cultured in osteogenic medium or basic culture medium for the osteogenic marker gene, osteocalcin (*OCN*), and *18S*.

Comparison of adipogenic differentiation potential of cells from different sources

Oil red O staining showed that cells cultured in control medium were not stained with oil red O to any extent. However, when cells from the different tissue sources were cultured in adipogenic medium and subsequently stained, microscopic assessment clearly revealed that lipid in the cells cultured in the adipogenic medium was stained with oil red O (data not shown). Furthermore, elution of associated oil red O revealed that SK cells cultured in adipogenic medium accumulated significantly more lipid (0.371 ± 0.065 optic density [OD]) than did SM (0.222 ± 0.083 OD) and SF cells (0.196 ± 0.054 OD) ($P < 0.05$). However, no differences were detected between SF, SM and BM cell populations with regard to adipogenesis.

Isolation and proliferative characterization of SF MSC/MPC clones

SF stem cell populations from each pig underwent limiting dilution analysis, and a total of 18 single-cell–derived clones (six from each animal) were randomly selected. Of the 18 clones, two reached 25–30 PDs, nine reached 30–35 PDs, five grew to 40–50 PDs and two reached beyond 50 PDs. The proliferation rates of these clones were assessed according to the time taken to reach 20 PDs (Figure 4). Variation in the proliferation rates was evident between clones, across animals and within the same animal. The time taken to reach 20 PDs ranged from 57–120 days, and the average rates (in days) to reach 20 PDs within each of animal A, B and C was 71.3 ± 12.0, 98.0 ± 13.3 and 74.7 ± 6.9, respectively (Figure 5). Cells from pig B demonstrated the slowest rates of proliferation and showed the most variation on the basis of both standard deviation (13.3) and the range, 37 days, to reach 20 PDs for this animal.

Clones were able to reach from 25–53 PDs and demonstrated linear growth kinetics up to 30 PDs.

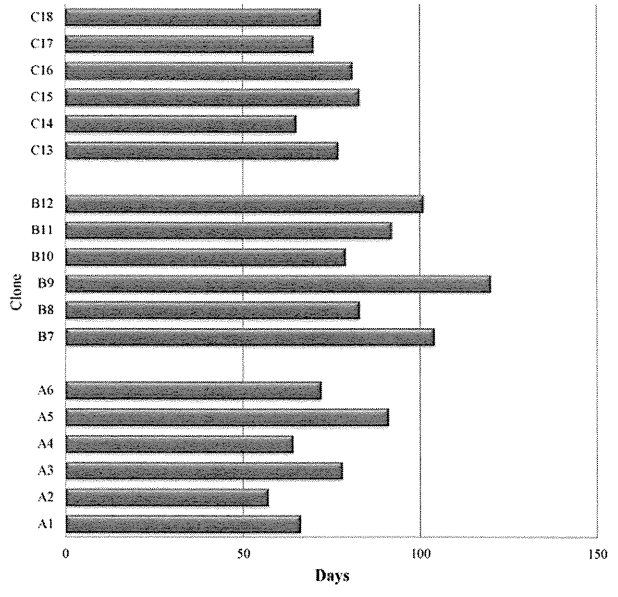

Figure 4. Proliferation rates for individual clonal populations to reach 20 PDs. Each bar represents the time taken, in days, for each clone to reach 20 PDs. Duration varied from 57–120 days to achieve 20 PDs. All clones were further analyzed for morphological changes and underwent phenotyping. On the y-axis, capital letter and numbers indicate the animals and corresponding clones.

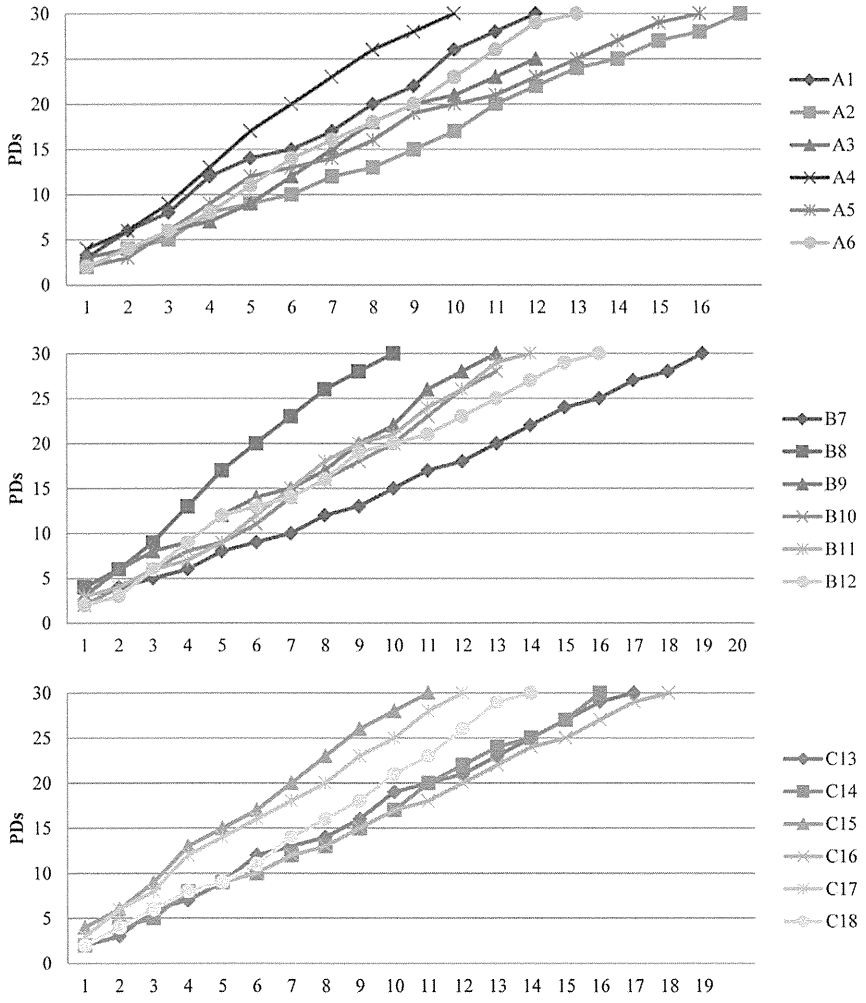

Figure 5. Kinetics of individual clones for growth up to 30 PDs. Kinetics were analyzed starting at the first passage. Cells from individual clones were plated at identical densities (3000/cm^2) on each passage, and total cell counts were assessed at each passage to calculate PDs. Growth curves overlapped and remained linear up to 30 PDs, with the exception of clone A3 and B10, which did not reach 30 PDs.

After this point, those that were able to expand further appear to have a progressive age-related decline in their growth rate as the result of the high number of expansions. Clone A2 demonstrated the highest rate, doubling its population every 2.85 days, whereas clone A9 took 6.0 days to double, with all other clones lying between these values. This variation was present within the same animal, as well as between animals. In pig B, clones doubled in population in as few as 3.96 days or required as many as 6.0 days. When grouping the clones according to their proliferation rate, the heterogeneity becomes very apparent. This was done by separating them into a high proliferative potential (HPP) group, medium proliferative potential group (MPP) and a low proliferative potential group (LPP), each containing six clonal populations, with the LPP containing the slowest proliferating cells. The HPP, MPP and LPP groups took on average 63.0 ± 4.1, 79.8 ± 2.8 and 104.3 ± 11.7 days to reach 20 PDs. Each of these groups was significantly different in the number of days it took reach 20 PDs; however, the total PDs that the HPP, MPP and LPP group were able to undergo were 38.5 ± 10.7, 35.3 ± 6.6 and 39.8 ± 9.5 PDs. The rates were significantly different with the different groups taking between 63 and 105 days to reach the same number of PDs but demonstrated no relationship with the total number of PDs (data not shown).

Histological stains

Alcian blue, a stain for glycosaminoglycans, was used as a qualitative measure of chondrocyte development. All 18 porcine-derived SF MSC clones differentiated into round, proteoglycan-producing chondrocytes, demonstrated by intense staining throughout the chondrocytes, which were numerous and spread across the plates. The small number of undifferentiated spindle-shaped cells remaining did not retain the alcian blue, confirming that the dye does not stain undifferentiated cells. When observed by means of

light microscopy, the extracellular matrix around the chondrocytes also stained with the dye.

Oil red O staining distinguishes lipid vacuole–containing cells from undifferentiated cells. Staining of differentiated adipogenic clones showed a large amount of variability in the quantity of vacuoles present but did show that SF MSCs have the ability to differentiate into adipocyte-like cells. Between 40–60% of the cells in each plate typically appeared as small spherical lipid–containing cells that stained intensely with oil red O. There was large variation within the clones from each animal regarding the extent of staining present. However, clones derived from pig A showed positive staining in up to 80% of cells but also lacked any staining in clones 2 and 4. There were also considerable differences between animals noted, in part because of to the large variation observed within each individual clone, and it was difficult to conclude that the animals themselves were different.

Alizarin red staining detects calcium deposition, which is an early step in osteogenesis. Seven of the clones exposed to the osteogenic medium showed widespread staining for calcium, and corresponding morphological changes were present in these seven clones after 21 days. The percentage of positively stained cells ranged from 0–40% within the 18 clones and is the first indication in a cell source that there may be limited potential for bone formation. Nonetheless, histological staining indicates that clonal SF MSCs are multipotent but could contain unique phenotypes that are biased toward cartilage formation.

Discussion

In the current studies, it has been demonstrated that porcine MSCs from various tissue sources show proliferation and differentiation characteristics similar to those reported in human MSCs (8,13). Such observations indicate that SF and SM MSCs probably are ideal candidate cell sources for future cartilage repair studies. Further analysis of SF MSC populations has demonstrated that heterogeneity exists at the clonal level as well but that "ideal" clonal populations may be identified that have enhanced propensity toward the chondrogenic lineage. These findings demonstrate that there may be unique phenotypes present in SF MSCs, setting the stage for future studies that may allow us to optimize our TEC model (10,11) through the use of highly characterized, and well-defined MSC populations.

Proliferation

The results presented in this report have demonstrated that adherent cells isolated from four different porcine sources exhibit osteogenic, chondrogenic and adipogenic differentiation potential and retain a similar proliferation potential up to at least passage 10.

Whereas cells from all sources exhibited multilineage potential, tissue-specific differences in the propensity to navigate down a specific lineage when exposed to suitable stimuli may indicate that these endogenous cells are primed to commit to one lineage versus another. SM MSCs have previously been reported to have significant chondrogenic differentiation potential in humans, as mentioned previously. However, this relationship has not been demonstrated previously across species, and, to develop an appropriate large animal model, these lineage-specific differences were analyzed in a porcine model because of physiological and chondrocyte similarities with humans (21).

In the present studies, SF MPCs exhibited a chondrogenic differentiation potential similar to SM MPCs *in vitro*. BM MPCs exhibited the greatest osteogenic differentiation potential among the examined 24 MPCs but significantly lower chondrogenic and adipogenic capacities. In a previous study, gene expression profiles of SF MSCs were reported to be similar to those of SM MSCs through the use of gene array approaches but different from those of BM MSC (22). This finding has been recently supported (23); however, our more limited RT-PCR analysis did not indicate such differences. In contrast, the present data suggest that SF MPCs and SM MPCs might be more committed to becoming differentiated chondrogenic progenitor cells, whereas BM MPCs might be more committed to becoming osteogenic progenitor cells, respectively. This conclusion/speculation may make teleological sense, given that the SF cells are in an intra-articular environment, in which they could migrate to damaged cartilage or cartilage in need of endogenous repair, whereas BM-associated cells could retain some chondrogenic potential but are mainly focused on bone repair and fracture healing because of their proximity.

Because the results of the differentiation capacity in this study are similar to results of a previous human study (8), the pig model may be a useful analogue for human studies to pursue continued pre-clinical understanding of this concept. As a result, further clonal analysis was completed of the SF MSCs to assess their potential for chondrogenesis. Their proliferative capacity was assessed, and their differentiation potential on the basis of standard histological staining techniques was analyzed to determine their feasibility as a source for cell therapies.

To develop standard protocols for expanding porcine SF MSCs, it was important to establish that they have additional fundamental MSC characteristics, such as proliferative capacity. Karystinou (24) previously reported that human SF MSCs have a

high self-renewal capacity inherent to the single cell, but, to our knowledge, this has not been examined in the porcine model, and SF MSCs have not been fully characterized in terms of their differentiation potential and as a viable candidate for cartilage repair. The MSCs isolated by means of limiting dilution demonstrated a high capacity for self-renewal. Only one clonal population was unable to reach 30 PDs (pig B, clone 10–28 PDs), and seven of 18 clones were able to expand beyond 40 PDs. These numbers fit within reported values for SM MSCs (24). Because significantly large numbers of cells are needed for cell therapies, such as the TEC approach, which has been demonstrated in a porcine model, this is a critical characteristic for any MSCs that would be used for this specific model or any other construct as well. The TEC protocol used by Ando *et al.* (10,11) requires approximately 4 million cells per well for a single construct. This would require approximately 22 PDs to get to this value from a single cell, emphasizing the importance of a high proliferative capacity because it probably would require 25 PDs or more to fully assess the biological and mechanical characteristics of these SF MSCs in a TEC model. The ability to predict self-renewal capacity has not been examined in SF MSCs but may be important because it has recently been documented that 10 of 50 clones isolated from human SM were unable to grow beyond 25 PDs (24) and thus may not be viable populations to use for tissue engineering. It would not be practical to expand so many populations at the same time with the use of current methods because of the numbers of flasks, growth media and labor hours required once cell numbers become high, nor would it be cost-efficient to expand cells that cannot reach the number necessary. Thus, we sought an approach to potentially predict the extent to which a population may be able to self-renew, on the basis of indications from proliferation rates at the earliest stages of expansion. The first five PDs were analyzed for each clonal population, and an initial proliferation rate was calculated on the basis of the time taken for each PD. The clones were separated into the five fastest (5F) and five slowest (5S) to determine whether there was a relationship with the total number of PDs. The 5F group took on average 3.04 ± 0.25 days per PD and reached a total of 39.0 ± 9.3 PDs, whereas the 5S group took 5.25 ± 0.4 days, reaching 39.8 ± 9.5 total PDs. Despite a significant difference in the initial growth rates, the capacity of the two distinct groups to proliferate was nearly identical. As such, there was no apparent correlation between the initial growth kinetics of SF MSCs and their overall capacity to expand *in vitro*. The lack of a relationship makes it difficult to predict their capacity for self-renewal. A similar lack of relationship of MSCs in human SM has also been reported (14). Important to note, however, is that the fastest proliferating cells do not appear to have a compromised differentiation capacity. This might indicate an ideal population to expand because less passaging and handling may be required, reducing the risk of *in vitro* artifacts occurring from extensive passaging, without compromising the differentiation potential of the cell population. Synovium-derived MSCs have been cultured in bioreactors (15), which could be a potential pathway to expanding these highly proliferating clonal populations for a more rapid turnaround for clinical applications.

Differentiation

When Pittenger *et al.* (25) examined six colonies of BM MSCs, they found that all six were osteogenic, five were adipogenic and two were chondrogenic. A year later, Muraglia *et al.* (26) expanded the study with 185 non-immortalized cell clones from bone marrow; 184 clones were osteogenic, with only one third differentiating into all three lineages, and those clones lost their adipogenic and chondrogenic potential progressively with passaging. This suggested that cells lose adipogenic and chondrogenic potential before that for osteogenic differentiation, as had been suggested by the absence of phenotypes expressing only chondro-adipo potential or separately. Of the 18 SF-derived MSCs analyzed in the present studies, two had a mono-potent chondrogenic potential, nine exhibited adipogenic-chondrogenic potential and seven were able to differentiate into all three lineages. This is the first time that this adiopogenic-chondrogenic phenotype has been reported in the literature. There was variation evident in the histological stains within the same the clonal populations. This may be a result of the clones being in different phases of their cell cycle when initially exposed to the differentiation medium. As MSCs differentiate, they typically generate an intermediate precursor or progenitor cell before becoming fully differentiated. Because we do not know exactly where in the cell cycle they are, there may be some variability as the result of this factor. In addition, it has been demonstrated that the microenvironment *in vitro* may induce epigenetic changes that can alter gene expression and ultimately control cell fate (26); however, this is beyond the scope of this report. Nonetheless, the chondrogenic ability of SF MSCs appears to be superior, which is consistent with the findings that SM MSCs also appear to have a predisposition for cartilage development. The absence of osteogenic potential has never been reported in any tissue, and this may be a beneficial characteristic unique to the SF. In some cases, BM MSCS have been reported to mineralize when used *in vivo* (27), but the

limited potential for bone formation may open possible avenues to explore where SF MSCs could circumvent this complication.

Limitations

Results from the current study demonstrated that ~40% of the isolated clonal MSCs were multipotent, typically lacking adipogenic potential. Pittenger (28) initially demonstrated that ~50% of mixed cell populations were inherently multipotent, whereas recent studies have demonstrated that possibly <20% of clonal MSC populations may be multipotent. This currently represents a major limitation in stem cell biology because it cannot currently be determined whether these populations previously had the ability to differentiate down multiple lineages when in their natural *in vivo* environment, which would indicate that this set of observations is an *in vitro* artifact. Recent theories also argue that the variation is reflective of the natural repertoire that these MSCs have and the multiple functions that they perform *in vivo* (29,30). Nonetheless, the impact of *in vitro* culturing and a lack of knowledge of the role that MSCs play in the natural repair process will continue to be limiting factors in the advancement of regenerative medicine. However, continued characterization of such cloned MSC, including a more complete analysis of gene expression patterns for a variety of molecules including transcription factors such as *Oct4* and Nanog (31), should allow for additional conclusions to be made regarding the potential of individual clones to initiate repair.

Relevance of SF-derived MSCs for future studies

MSCs are routinely isolated from SM by digestion of this tissue with animal-derived collagenase. However, in April 2007, the United States Food and Drug Administration indicated a potential risk for introduction of transmissible spongiform encephalopathy agents into the process for cell isolation through the use of commonly used collagenase preparations (32). Because cells destined for clinical applications must be handled in compliance with current good tissue practice and Good Manufacturing Practice regulations, the use of animal-derived collagenase poses a significant hurdle (33). Whereas alternate sources of collagenase are available, including a Good Manufacturing Practice–grade collagenase, these collagenases are significantly more expensive and are also manufactured with animal products; therefore, their use does not eliminate the potential risk of contamination with transmissible spongiform encephalopathy agents. Thus, other sources of cells that can be isolated without collagenase treatment but still exhibit comparable chondrogenic differentiation potential to SM-derived MSCs are desirable for the development of safe cell therapy approaches to initiate cartilage repair. Therefore, SF MPCs are not only the most chondrogenic progenitor cell populations, they can also be isolated without collagenase after elimination of as many risks as possible for subsequent cell use. Thus, these cells should be considered desirable sources of clinical cell-based therapy for cartilage in terms of efficacy and safety.

Relevance of porcine studies to human applications

The pig is widely used as the "ideal" preclinical model for many human conditions because it has a physiology very similar to humans (eg, widely used in cardiovascular studies) (34). It is a large-animal model with a knee similar in size to a human knee [eg, can be used for transplantation of tissue-engineered cartilage or menisci derived from MSCs (10,35–37) as a precursor to attempting such transplants into human knees], and the MSCs derived from pig SMs are very similar to those from humans (11). Furthermore, a number of investigators and companies have been generating more "humanized" pigs (through genetic manipulations to remove specific glycosyl transferases and other gene products) for consideration for use as a source for organs to transplant into humans (37). Although such approaches have a number of obstacles to overcome and challenges to meet, it does demonstrate that many researchers consider the pig as an excellent model for humans, with good potential for translation to humans from this preclinical model.

Conclusions

Cell therapies are currently being used as a method of cartilage repair; however, because of unstable phenotypes, there are still many limitations in the field. We have demonstrated that SF MSCs in pigs share characteristics similar to that in humans and may be a superior source of MSCs. The reported studies have demonstrated high potential for proliferation, and initial results suggest an enhanced potential for chondrogenesis. SF could provide an accessible source of autologous MSCs; however, further analysis must be performed to determine if highly characterized and stable phenotypes can be isolated. This could provide cells with optimal properties for specific complications, and the porcine model may be ideal to further assess this possibility.

Acknowledgments

The authors acknowledge the Canadian Institute of Health Research (CIHR), Alberta Innovates Health Solutions (Osteoarthritis Interdisciplinary Team

Grant) and the Canadian Arthritis Society for financial support.

Disclosure of interests: The authors have no commercial, proprietary, or financial interest in the products or companies described in this article.

References

1. Brittberg M, Peteron L, Sjouml Gren-Jansson E, Tallheden T, Lindahl A. Articular cartilage engineering with autologous chondrocyte transplantation: a review of recent developments. J Bone Joint Surg. 2003;85:109–15.
2. Peterson L, Minas T, Brittberg M, Nilsson A, Sjogren-Jansson E, Lindahl A. Two-to 9-year outcome after autologous chondrocyte transplantation of the knee. Clin Orthop Relat Res. 2000;374:212–34.
3. Roberts S, Hollander A, Caterson B, Menage J, Richardson J. Matrix turnover in human cartilage repair tissue in autologous chondrocyte implantation. Arthritis Rheum. 2001;44:2586–98.
4. Dell'Accio F, De Bari C, Luyten F. Molecular markers predictive of the capacity of expanded human articular chondrocytes to form stable cartilage in vivo. Arthritis Rheum. 2001;44:1608–19.
5. Saleh F, Whyte M, Genever P. Effects of endothelial cells on human mesenchymal stem cell activity in a three-dimensional in vitro model. Eur Cell Mater. 2011;22:242–57.
6. Ando W, Heard B, Chung M, Nakamura N, Frank C, Hart DA. Ovine synovial membrane-derived mesenchymal progenitor cells retain the phenotype of the original tissue that was exposed to in-vivo inflammation: evidence for a suppressed chondrogenic differentiation potential of the cells. Inflamm Res. 2012;61:1–10.
7. Krawetz R, Wu YE, Martin L, Rattner JB, Matyas JR, Hart DA. Synovial fluid progenitors expressing CD90+ from normal but not osteoarthritic joints undergo chondrogenic differentiation without micro-mass culture. PloS One. 2012;7: e43616.
8. Sakaguchi Y, Sekiya I, Yagishita K, Muneta T. Comparison of human stem cells derived from various mesenchymal tissues: superiority of synovium as a cell source. Arthritis Rheum. 2005;52:2521–9.
9. Nakamura T, Sekiya I, Muneta T, Hatsushika D, Horie M, Tsuji K, et al. Arthroscopic, histological and MRI analyses of cartilage repair after a minimally invasive method of transplantation of allogeneic synovial mesenchymal stromal cells into cartilage defects in pigs. Cytotherapy. 2012;14:327–38.
10. Ando W, Tateishi K, Hart DA, Katakai D, Tanaka Y, Nakata K, et al. Cartilage repair using an in vitro generated scaffold-free tissue-engineered construct derived from porcine synovial mesenchymal stem cells. Biomaterials. 2007;28: 5462–70.
11. Ando W, Tateishi K, Katakai D, Hart DA, Higuchi C, Nakata K, et al. In vitro generation of a scaffold-free tissue-engineered construct (TEC) derived from human synovial mesenchymal stem cells: biological and mechanical properties and further chondrogenic potential. Tissue Eng: Part A. 2008; 14:2041–9.
12. Schellenberg A, Stiehl T, Horn P, Joussen S, Pallua N, Ho AD, Wagner W. Population dynamics of mesenchymal stromal cells during culture expansion. Cytotherapy. 2012;14:401–11.
13. De Bari C, Dell'Accio F, Tylzanowski P, Luyten F. Multipotent mesenchymal stem cells from adult human synovial membrane. Arthritis Rheum. 2001;44:1928–42.
14. De Bari C, Dell'Accio F, Karystinou A, Guillot P, Fisk N, Jones E, et al. A biomarker-based mathematical model to predict bone-forming potency of human synovial and periosteal mesenchymal stem cells. Arthritis Rheum. 2008;58: 240–50.
15. Reno C, Marchuk L, Sciore P, Frank CB, Hart DA. Rapid isolation of total RNA from small samples of hypocellular dense connective tissues. Biotechniques. 1997;22:1082–6.
16. Dry H, Jorgensen K, Ando W, Hart DA, Frank CB, Sen A. Effect of calcium on the proliferation kinetics of synovium-derived mesenchymal stromal cells. Cytotherapy. 2013;15: 1–15.
17. Hellio Le Graverand MP, Reno C, Hart DA. Heterogeneous response of knee cartilage to pregnancy in the rabbit: assessment of specific mRNA levels. Osteoarthritis Cartilage. 2000; 8:53–62.
18. Jiang Y, Mishima H, Sakai S, Liu YK, Ohyabu Y, Uemura T. Gene expression analysis of major lineage-defining factors in human bone marrow cells: effect of aging, gender, and age-related disorders. J Orthop Res. 2008;26:910–7.
19. Lu T, Achari YA, Rattner JB, Hart DA. Evidence that estrogen receptor β enhances MMP-13 promoter activity in HIG-82 cells and that this enhancement can be influenced by ligands and involves specific promoter sites. Biochem Cell Biol. 2007;85:326–36.
20. Zou L, Zou X, Chen L, Li H, Mygind T, Kassem M, et al. Multilineage differentiation of porcine bone marrow stromal cells associated with specific gene expression pattern. J Orthop Res. 2008;26:56–64.
21. Schulze-Tanzil G, Müller RD, Kohl B, Schneider N, Ertel W, Ipaktchi K, et al. Differing in vitro biology of equine, ovine, porcine and human articular chondrocytes derived from the knee joint: an immunomorphological study. Histochem Cell Biol. 2009;131:219–29.
22. Magari K, Nishigaki F, Sasakawa T, Ogawa T, Miyata S, Ohkubo Y, et al. Anti-arthritic properties of FK506 on collagen-induced arthritis in rats. Inflamm Res. 2003;52:524–9.
23. Horie M, Sekiya I, Muneta T, Ichinose S, Matsumoto K, Saito H, et al. Intra–articular injected synovial stem cells differentiate into meniscal cells directly and promote meniscal regeneration without mobilization to distant organs in rat massive meniscal defect. Stem Cells. 2009;27:878–87.
24. Karystinou A, Dell'Accio F, Kurth TB, Wackerhage H, Khan IM, Archer CW, et al. Distinct mesenchymal progenitor cell subsets in the adult human synovium. Rheumatology. 2009;48:1057–64.
25. Pittenger M, Mackay AM, Beck SC, Jaisal RK, Douglas R, Mosca JD, et al. Multilineage potential of adult human mesenchymal stem cells. Science. 1999;284:143–7.
26. Arnsdorf EJ, Tummala P, Castillo AB, Zhang F, Jacobs CR. The epigenetic mechanism of mechanically induced osteogenic differentiation. J Biomech. 2012;43:2881–6.
27. Muraglia A, Cancedda R, Quarto R. Clonal mesenchymal progenitors from human bone marrow differentiate in vitro according to a hierarchical model. J Cell Sci. 2000;113: 1161–6.
28. Hashemi SM, Ghods S, Kolodgie FD, Parcham-Azad K, Keane M, Hamamdzic D, et al. A placebo controlled, dose-ranging, safety study of allogenic mesenchymal stem cells injected by endomyocardial delivery after an acute myocardial infarction. Eur Heart J. 2008;29:251–9.
29. Chen FG, Zhang WJ, Bi D, Liu W, Wei X, Chen FF, et al. Clonal analysis of nestin–vimentin+ multipotent fibroblasts isolated from human dermis. J Cell Sci. 1999;120(Pt 16):2875–83.
30. Pevsner-Fischer M, Levin S, Zipori D. The origins of mesenchymal stromal cell heterogeneity. Stem Cell Rev Rep. 2011;7:560–8.